Cysteine trisulfide oxidizes protein thiols and induces electrophilic stress in human cells

Christopher H. Switzer [a],[*], Sebastian Guttzeit [a], Thomas R. Eykyn [b], Philip Eaton [a],[**]

[a] William Harvey Research Institute, Barts and the London School of Medicine and Dentistry, Queen Mary University of London, London, UK
[b] School of Biomedical Engineering & Imaging Sciences, King's College London, London, UK

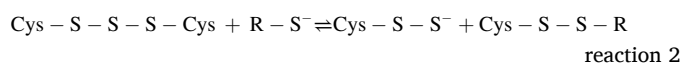| ARTICLE INFO	ABSTRACT
	The cellular effects of hydrogen sulfide (H_2S) signaling may be partially mediated by the formation of alkyl persulfides from thiols, such as glutathione and protein cysteine residues. Persulfides are potent nucleophiles and reductants and therefore potentially an important endogenous antioxidant or protein post-translational modification. To directly study the cellular effects of persulfides, cysteine trisulfide ($Cys-S_3$) has been proposed as an *in situ* persulfide donor, as it reacts with cellular thiols to generate cysteine persulfide ($Cys-S-S^-$). Numerous pathways sense and respond to electrophilic cellular stressors to inhibit cellular proliferation and induce apoptosis, however the effect of $Cys-S_3$ on the cellular stress response has not been addressed. Here we show that $Cys-S_3$ inhibited cellular metabolism and proliferation and rapidly induced cellular- and ER-stress mechanisms, which were coupled to widespread protein-thiol oxidation. $Cys-S_3$ reacted with Na_2S to generate cysteine persulfide, which protected human cell lines from ER-stress. However this method of producing cysteine persulfide contains excess sulfide, which interferes with the direct analysis of persulfide donation. We conclude that cysteine trisulfide is a thiol oxidant that induces cellular stress and decreased proliferation.

1. Introduction

Endogenous and pharmacologically derived H_2S have shown beneficial effects in multiple disease models [1–3]; however its cellular signaling mechanisms are not well understood. A potential mechanism of H_2S signaling is the formation of persulfides from oxidized cellular thiol species, such as disulfides, sulfenic acids, nitrosothiols, and polysulfides (reaction 1) [4,5].

$$HS^- + R-S-X \rightleftharpoons R-S-S^- + HX \ (X = -OH, \ -(S)_nR/H, \ -NO)$$

reaction 1
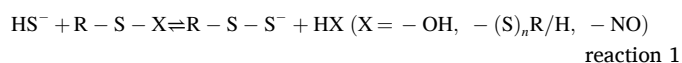
For example, H_2S reacts with cystine or glutathione disulfide to form cysteine or glutathione persulfide [1,6]. Additionally, cysteine persulfide is enzymatically generated by cysteinyl-tRNA synthetase [7–9]. Due to the alpha effect [10], persulfides are more nucleophilic than thiols [6,11,12] and have shown cellular protective effects and antioxidant function [12–14]. Persulfides can transfer the terminal sulfur to other thiols in a *trans*-sulfuration reaction [8,15,16]. The *trans*-sulfuration of

protein cysteine residues may alter enzyme activities [17,18] or confer a gain of function, such as the cyanide metabolizing function of persulfide-modified thiosulfate sulfurtransferase [19]. Therefore the chemical biology of H_2S is interconnected with persulfide formation and reactivity.

There are limited methods to directly investigate cellular persulfides due to the highly reactive nature and complex equilibria between persulfides and related thiol species [7,13,20,21]. Protein persulfides have been made from reacting 5,5'-dithio-bis-(2-nitrobenzoic acid) with cysteine and then H_2S [1,22]. Thiol-sepharose persulfide has also been used to explore persulfide reactivity [12]. However these tools are not suitable for *in vitro* cellular or *in vivo* experimentation. $Cys-S_3$ has been utilized as a cellular persulfide donor by reacting with intracellular thiols (reaction 2) [13,23,24].

$$Cys-S-S-S-Cys + R-S^- \rightleftharpoons Cys-S-S^- + Cys-S-S-R$$

reaction 2

While these studies have focused on the effects of persulfide

formation [13,24], the oxidation of cellular thiols by Cys-S$_3$ has not been examined. Cells respond to electrophilic stress by cysteine-mediated sensing molecules such as p38, KEAP1 and PDIs [25–27]. While Cys-S$_3$ has been shown to protect cells from further electrophilic insult [13,24], the cellular effect of the electrophile Cys-S$_3$ on cellular and endoplasmic reticulum (ER) stress has not been investigated. Here we show that despite forming cysteine persulfide, Cys-S$_3$ also results in global protein thiol oxidation, the induction of cellular and ER-stress responses and inhibited cell proliferation. However, pre-reacting Cys-S$_3$ with excess sulfide at high pH yielded a stable solution of cysteine persulfide, which did not induce cell stress or protein oxidation. Furthermore, Cys-SS$^-$ produced from Cys-S$_3$ and sulfide prevented thapsigargin-induced ER-stress, however the presence of excess sulfide limits the interpretation of persulfide effects on electrophile-induced ER-stress. Therefore we conclude that Cys-S$_3$ induces a toxic cellular response with concomitant persulfide generation.

2. Materials and methods

2.1. Chemicals and reagents

Cysteine trisulfide was generously synthesized and provided by Prof Jon M. Fukuto (Sonoma State University) and was >90% pure by ^{1}H NMR and ESI-MS and the major impurity was cystine [13]. Cysteine trisulfide stock solutions were made in 10 mM HCl unless otherwise specified and used immediately. 4,4′-dipyridyl disulfide, cystine, dithiothreitol, sodium sulfide (Na$_2$S), sodium hydrosulfide (NaSH), oxidized glutathione and Thapsigargin were obtained from Sigma-Aldrich. Phosphate buffered saline, distilled water and bio-tinylated glutathione ethyl ester (BioGEE) was obtained from Invitrogen and bond-breaker TCEP solution and monobromobimane was from ThermoFisher.

2.2. Cell culture and proliferation

HEK293, RAMOS and Jurkat human cell lines were obtained from ATCC. Cells were cultured in RPMI supplemented with 10% fetal calf serum and pen/strep. Cells were passaged and cultured at 37°C 5% CO$_2$ atmosphere. Cell viability and counting was performed on Countess II automated cell counter (Invitrogen). RAMOS and Jurkat cells were cultured between 0.2 and 2.0e6 cells/ml. HEK cells were passaged 2–3 times per week with warm trypsin (Invitrogen). Cell proliferation was measured by electrical impedance using an xCelligence RTCA DP analyzer (Agilent) with E-plate 16 glass plates. HEK293 cells were harvested and counted and further diluted into E-plate 16 wells in 100 μL media. Cys-S$_3$ or Cys-SS$^-$ was added (1:100 dilution) to wells and plates were loaded into the analyzer in a humidified, 5% CO$_2$ incubator at 37°C. Cell index measurements were recorded every 15 min and normalized to wells containing media without cells.

2.3. GSH oxidation

Cys-S$_3$ (10 mM) and GSH (50 mM) stock solutions were made in 10 mM NaOH. Cys-S$_3$ was added to equal volume 10 mM NaOH or 50 mM GSH and incubated for 10 min at room temperature. UV–visible absorption data were obtained on a Picodrop 200 spectrophotomer with a standard quartz microcuvette blanked with 10 mM NaOH. Data shown are representative of 4 independent reactions. First derivative of delta absorbance values were calculated with Graphpad Prism 9 software.

2.4. PKGIα expression and purification

FreeStyle 293-F cells (Invitrogen) were transfected with pcDNA3-hPKGIα-His-V5 (3 μg/ml) and polyethylenimine (9 μg/ml) and cultured in serum-free Gibco FreeStyle 293 Expression Media (Thermo Fisher) supplemented with 2.2 mM valporic acid 24 h after transfection and cultured for 6 days. Cleared cell lysate (25 mM sodium phosphate, 100 mM NaCl and cOmplete™ mini, EDTA-free protease inhibitor, pH 7) was incubated with Ni-NTA slurry at 4 °C for 3 h, added to a gravity puri-fication column and washed using 20 vol washing buffer containing 25 mM sodium phosphate, 1 mM NaCl, 40 mM imidazole, pH 7, followed by 5 vol 25 mM sodium phosphate, 300 mM NaCl, 40 mM imidazole, pH 7. Subsequent elutions were collected in 2 ml fractions using a buffer containing 25 mM sodium phosphate, 300 mM NaCl, 500 mM imidazole, pH 7. Pooled fractions were dialysed using Slide-A-Lyzer™ cassettes (10 kDa cut off) (ThermoFisher) against 25 mM sodium phosphate, 50 mM NaCl, pH 7 and loaded on a HiTrap Q HP anion exchange chromatog-raphy column (GE Life Science) and washed with 10 vol of low salt buffer containing 25 mM sodium phosphate, 50 mM NaCl, pH 7. Protein was eluted using a stepwise increase in NaCl concentration (100–500 mM). Protein containing fractions were pooled and dialysed using Slide-A-Lyzer™ cassettes (10 kDa cut off) (ThermoFisher) against 25 mM sodium phosphate, 300 mM NaCl and pH 7 and stored at −80 °C.

2.5. Purified PKGIα oxidation

Purified PKGIα (1 μM) in Tris buffer (50 mM, pH 7.5) was treated with TCEP (250 μM) for 1 h at 37°C and excess TCEP was removed with a Zeba desalting spin column. TCEP-reduced PKGIα was then incubated with Cys-S$_3$ (100 μM) for 30 min 37°C and PKGIα was purified with a Zeba desalting spin column. Cys-S$_3$ oxidized PKGIα was then incubated with DTT for 60 min 37°C. Reaction aliquots were mixed with equal volumes of 2X SDS sample buffer containing 50 mM maleimide and heated to 85°C for 10 min with agitation.

2.6. Western blotting

Cells were treated with Cys-S$_3$, NaSH or Cys-SS$^-$ in RPMI growth media for the indicated times at 37°C, washed with PBS and lysed with 2X SDS sample buffer containing 5% 2-mercaptoethanol or 2X SDS sample buffer containing 50 mM maleimide was used for non-reducing immunoblots. Lysates were heated to 85°C with 1500-rpm agitation for 10 min. Lysates and molecular weight marker were then separated on 4–20% gradient polyacrylamide tris-glycine gels with constant voltage. Gels were transferred to PVDF membranes using Trans-Blot Turbo Transfer System (Bio-Rad) and blocked with 5% BSA in PBS containing 0.1% Tween 20. Membranes were then incubated with primary antibody overnight at 4°C, washed and incubated with secondary for 1 h at room temperature. HRP was detected by briefly incubating membranes in ECL solution and exposure to x-ray film or iBright FL1500 imaging system. Fluorescent-tagged secondary antibodies were detected using an iBright FL1500 imaging system. Density of bands were determined by Gel-Pro software and normalized to controls. Antibody source and final di-lutions used in this study are listed in Supplemental Table 1.

2.7. Protein S-glutathiolyation

Cells were suspended in RPMI growth media containing vehicle (10 mM HCl) or Cys-S$_3$ and incubated for 30 min at 37°C. Cells were collected, washed with PBS and incubated in RPMI growth media con-taining BioGEE and incubated 30 min at 37°C. Cells were collected and washed with PBS and then lysed with 2X SDS sample buffer containing 50 mM maleimide. Biotinylated proteins were then detected as above with streptavidin-HRP (1:10,000 dilution, 1 h at room temperature).

2.8. Cell viability and toxicity measurements

Cell viability was determined by MTS reduction using the CellTiter 96® AQueous One Solution Cell Proliferation Assay as recommended by manufacturer's instructions with RPMI +10% FBS as a blank reading. Cell toxicity was determined by trypan blue staining. Cells were washed with PBS and incubated at a 1:1 ratio with 4% trypan blue solution

(InVitrogen) for 5 min. Trypan-positive and trypan-negative cell populations were determined on a Countess™ II Automated Cell Counter (InVitrogen).

2.9. Cellular glutathione measurements

Cellular reduced/oxidized glutathione measurements were performed using the GSH-Glo™ Glutathione Assay (Promega, #V6911) as instructed. Briefly, cells were lysed in the presence of glutathione-S-transferase (GST) and luciferin-NT substrate to form luciferin, which was detected by luciferase-generated luminescence to determine reduced glutathione. The samples are then incubated with TCEP (1 mM) for 30 min at 37°C and assayed as above. Luminescence was measured on a CLARIOstar plate reader (2 s integration per well).

2.10. Media thiol measurements

Reduced thiol concentration in media was determined by mBBr fluorescence and compared to a cysteine standard curve. mBBr stock solution (10 mM in DMSO) was diluted to 0.1 mM into 200 µL RPMI + 10% FBS or cysteine standards and incubated for 10 min at 37°C. Relative fluorescence units were then recorded on a CLARIOstar plate reader (ex. 394/em. 490 nm) and media without mBBr was used as a blank control. Media thiol content was calculated from a cysteine standard curve from 6 independent measurements.

2.11. Persulifde spectroscopy and kinetics

Sodium sulfide and cysteine trisulfide stock solutions were made in 10 mM NaOH and used immediately. A quartz microcuvette was blanked with 10 mM NaOH. Cys-S$_3$ was added to the cuvette with equal volume of NaSH and UV–visible spectra recorded with a Picodrop spectrophotometer. Reaction of 4,4′-dipyridyl disulfide with sodium sulfide, Cys-S$_3$ or Cys-SS$^-$ was measured on a CLARIOstar plate reader. The formation of 4-pyridinethiol was monitored after the injection of 4,4′-dipyridyl disulfide dissolved in ethanol. Linear and nonlinear regression analyses, initial rates and goodness of fit were calculated by Graphpad Prism 9.

2.12. Cellular microscopy and lactate measurements

Cells were cultured for 4 days in the presence of vehicle (10 mM HCl), Cys-S$_3$ or Cys-SS$^-$ in 6-well plates. Plates were mounted onto EVOS M7000 imaging system (ThermoFisher Scientific) and bright field images were recorded at 20X magnification. Used media and control media (incubated without cells) were then removed from wells, passed through 0.22 µm filters and stored at −80°C until NMR analysis. Filtered conditioned media were analyzed for lactate by ^{1}H NMR as previously described [28].

2.13. Thapsigargin-mediated ER-stress

Cys-SS$^-$ was synthesized as above, diluted into RPMI media and added to cell pellets. Thapsigargin was then diluted into the cell suspension (1 µM final concentration) and incubated for 30 min at 37°C. Cell pellets were formed (3 min, 250×g) and 2x SDS sample buffer containing either 5% 2-ME or 100 mM maleimide was added and analyzed as described above.

2.14. Statistical analyses

All statistical comparisons and corresponding p values were calculated by either two-tailed unpaired t-test or one-way ANOVA with Dunnet's post-hoc test by Graphpad Prism 9. Calculated p-values less than 0.05 were determined to be statistically significant and indicated on graphs. Linear or pseudo-first order curve fitting and goodness of fit

(r^2) were calculated by Graphpad Prism 9 and indicated in figure legends.

3. Results

3.1. Cysteine trisulfide oxidizes protein thiols

In situ persulfide generation from Cys-S$_3$ requires a nucleophile to break a trisulfide S–S bond (reaction 2). To verify that Cys-S$_3$ reacts with cellular thiols to form cysteine persulfide, glutathione (GSH) was reacted with Cys-S$_3$. The resulting product had an absorption peak at 340 nm (Fig. 1A and Supplemental Fig. 1) and showed increased initial reaction rates with 4,4′-dipyridyl disulfide compared to GSH alone (Supplemental Fig. 2), consistent with persulfide formation [1,11,29]. Therefore cysteine trisulfide oxidizes thiols to form persulfides in our hands. To determine if Cys-S$_3$ reacts with protein thiols, the oxidation of purified human cGMP-dependent protein kinase-1 (PKGIα) was examined [30]. PKGIα was isolated as the air-oxidized dimer, which was reduced by TCEP to the monomeric form (Fig. 1B). PKGIα monomer was then reacted with Cys-S$_3$, which resulted in oxidation to the dimer species. The Cys-S$_3$-treated dimer was further reduced back to the monomeric state by DTT, indicating that Cys-S$_3$ induced a reversible oxidation of PKGIα cysteine-42. To determine if Cys-S$_3$ caused PKGIα oxidation in cells, HEK293 and RAMOS cells were treated with Cys-S$_3$ for 30 min and lysates were analyzed by non-reducing immunoblotting. Cys-S$_3$ caused a concentration-dependent increase in PKGIα oxidized dimer compared to vehicle controls (Fig. 1C and Supplemental Fig. 3). Similarly, Cys-S$_3$ also caused a concentration-dependent oxidation of PTEN. PTEN dimer was formed with 10 µM Cys-S$_3$ and decreased as Cys-S$_3$ concentrations increased, while the intra-molecular di/trisulfide bond, which migrates lower on PAGE gels [31], was present at 10 µM Cys-S$_3$ and peaked at 100 µM (Fig. 1D). At 1 mM Cys-S$_3$, PTEN predominately appears as high molecular weight aggregates. These results suggest that Cys-S$_3$ oxidized PTEN, first forming the dimer, then the intra-molecular di/trisulfide and finally forming protein aggregates. Oxidation of PTEN is associated with the inhibition of phosphatase activity and is therefore predicted to increase Akt phosphorylation and activity. However, Cys-S$_3$ did not result in the activation of Akt despite PTEN oxidation (Supplemental Fig. 4). Cys-S$_3$ also resulted in a KEAP1 molecular weight complex consistent with dimerization at 10 and 100 µM and aggregation at 1 mM in RAMOS cells (Fig. 1E), further indicating that Cys-S$_3$ acts as a thiol oxidant in cells. Additionally, Cys-S$_3$ induced cellular protein oxidation was observed after only 10 min and protein oxidation persisted after 1 h (Supplemental Fig. 5), indicating that Cys-S$_3$ rapidly oxidizes protein thiols and that the oxidation is not readily resolved.

The presence of thiol species in serum-replete media may cause an extracellular reaction with Cys-S$_3$, which may alter the cellular effects observed. However, thiols are readily oxidized to disulfides by transition metal ions (*e.g.*, Fe^{3+}) in synthetic media and we determined that <600 nM of reactive thiols are present in cell culture media containing 10% fetal bovine serum (Supplemental Fig. 6A). Furthermore, Cys-S$_3$-mediated oxidation of PKG and PTEN were identical in cells treated in serum-containing RPMI or PBS (Supplemental Fig. 6B). Therefore we conclude that Cys-S$_3$ does not appreciably react with thiols in the media and the effects observed in cells are due to trisulfide reactivity.

Protein thiol oxidation in cells results in S-glutathionylation [32]. To further detect oxidized protein thiols in cells treated with Cys-S$_3$, biotin-conjugated glutathione ethyl ester (BioGEE) was added to HEK293 cells after exposure to Cys-S$_3$ or vehicle. Cys-S$_3$ caused a marked increase in S-glutathionylated proteins compared to vehicle controls as detected by non-reducing blotting (Fig. 1F). Similarly, Cys-S$_3$ caused a significant decrease of the reduced/oxidized glutathione ratio compared to vehicle control treated HEK293 cells (Supplemental Fig. 7). These data indicate that Cys-S$_3$ induced rapid and widespread protein thiol oxidation in human cell lines.
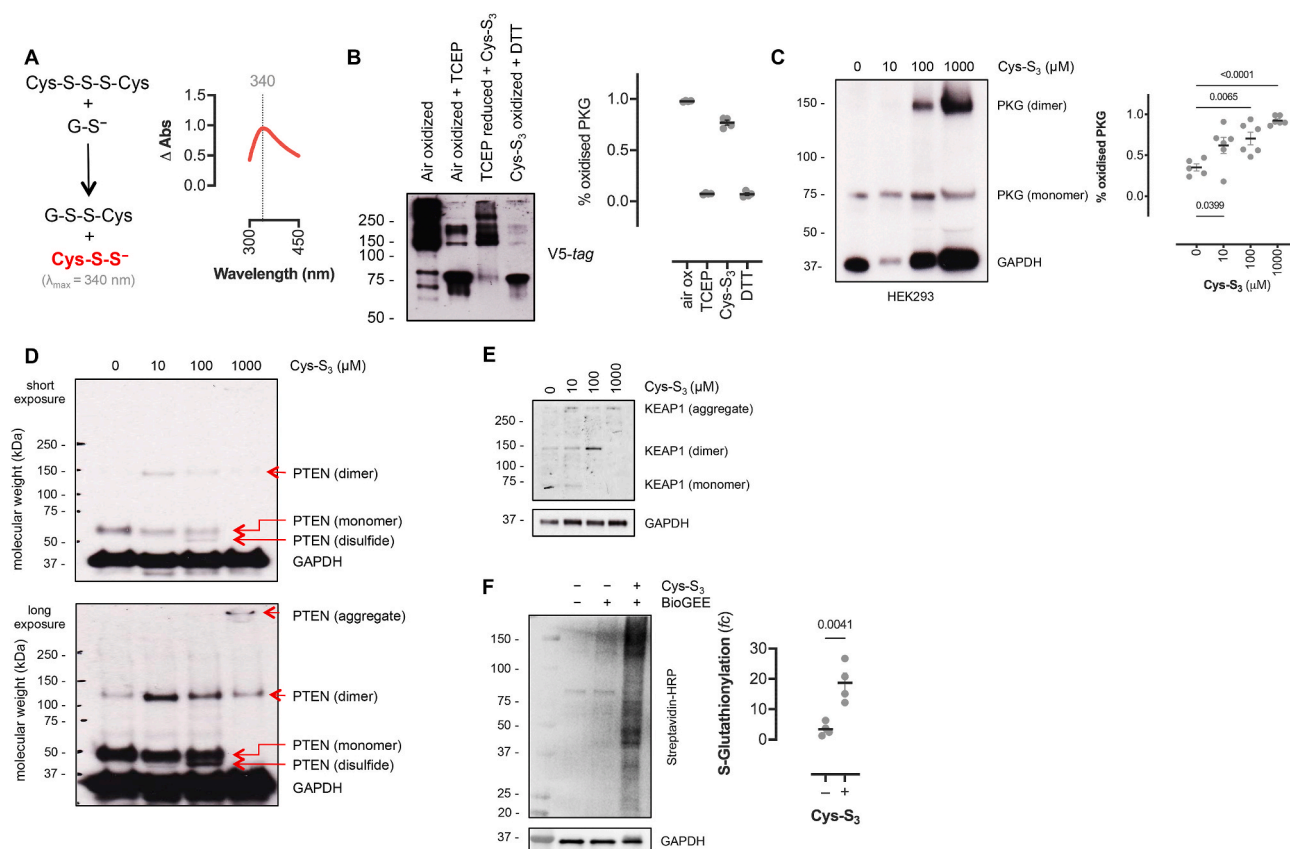
Fig. 1. Cysteine trisulfide oxidizes cellular protein thiols. (A) Differential absorption spectrum of Cys-SS− formed from Cys-S3 (5 mM) and GSH (25 mM), with a local maximum of 340 nm. (B) Non-reducing immunoblot of purified, air oxidized V5-tagged human PKG (lane 1), air oxidized PKG + TCEP (lane 2), TCEP-reduced PKG + Cys-S3 (lane 3) and Cys-S3-oxidized PKG + DTT. Graph represents mean fraction of oxidized PKG (±sem; n = 4). (C) Non-reducing immunoblot of PKG and GAPDH from HEK293 cells treated with Cys-S3 for 30 min. Graph represents mean fraction of oxidized PKG (±sem; n = 6). Significance was calculated by one-way ANOVA with Dunnett's post-hoc test. (D–E) Non-reducing immunoblot of PTEN (D) or KEAP1 (E) and GAPDH from RAMOS cells treated with Cys-S3 for 30 min. (F) Non-reducing immunoblot of S-glutathionylated proteins and GAPDH from HEK293 cells treated with or without Cys-S3 (100 μM) and BioGEE compared to untreated cells. Graph shows mean BioGEE intensity fold-change (±sem; n = 4) compared to control. Significance was calculated by two-tailed, unpaired *t*-test.

3.2. Cysteine trisulfide induces cellular and ER-stress

Protein thiol oxidation is coupled to the cellular stress response [33]. To examine if Cys-S3 treatment induced cellular stress signaling, p38-MAPK and stress-activated protein kinase (SAPK) pathway activation was measured in HEK293 and RAMOS cells. Cys-S3 resulted in the phosphorylation of both p38 and SAPK (Fig. 2A and Supplemental Fig. 8), indicating that Cys-S3 induces cellular stress responses. To examine if Cys-S3 also induced ER stress, eIF2α phosphorylation was measured. Cys-S3 caused significant eIF2α phosphorylation in both cell lines (Fig. 2B), indicating that Cys-S3 induced both cellular- and ER-stress pathways. Additionally, Cys-S3 induced significant IRE1α phosphorylation and caspase-2 cleavage, similar to thapsigargin controls, indicating that Cys-S3 induces pro-apoptotic ER-stress signaling (Supplemental Fig. 9). ER stress is associated with decreased protein synthesis and cellular proliferation and is induced by electrophilic stress [34]. To determine if Cys-S3 effects cellular proliferation, HEK293 cell growth was monitored via electrical impedance. Consistent with ER- and cellular-stress, Cys-S3 inhibited cellular proliferation (Fig. 2C) and lactate production (Fig. 2D). Similarly, Cys-S3 resulted in decreased cellular viability and increased cellular toxicity in both HEK293 and RAMOS cell lines (Supplemental Fig. 10). Furthermore, the morphology of Cys-S3-treated HEK293 cells was distinctly altered compared to vehicle-treated cells and resemble apoptotic cellular debris (Supplemental Fig. 11). Therefore, we conclude that Cys-S3 induces global protein thiol oxidation, cellular and ER stress-induced apoptosis, and inhibited cellular metabolism and proliferation. This indicates that

persulfide generation does not limit the cellular effects of the electrophilic stress that occurs concomitantly with persulfide formation.

3.3. Cysteine trisulfide reacts with sulfide to form cysteine persulfide

The electrophilic nature of Cys-S3 limits its use as a persulfide donor in human cell lines. However, prior reaction with extra-cellular or exogenous thiols is predicted to alleviate the ER- and cellular-stress induced by Cys-S3, as shown in reaction 2. However if the sacrificial nucleophile is sulfide, two equivalents of Cys-SS− are the only predicted product, as shown in reaction 3. The reverse reaction would be minimized at high pH conditions and the only product is persulfide as opposed to reaction 2.

$$Cys - S - S - S - Cys + H - S^- \rightleftharpoons 2Cys - S - S^- + H^+ \qquad \text{reaction 3}$$
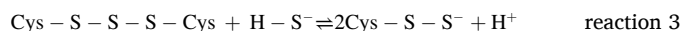
Increasing concentrations of Na2S were added to 5 mM Cys-S3 in 10 mM NaOH, which resulted in Cys-SS− formation (λ_{max} = 340 nm) (Fig. 3A). The equilibrium dissociation constant (reaction 3) was calculated to be ~2.4 fold Cys-S3 for these reaction conditions (Fig. 3B). The rate of persulfide formation was examined at 10-fold sulfide (Fig. 3C) and the half-life of Cys-S3 under these conditions was 29 s and equilibrium was established after ~2–3 min (Fig. 3D). Cysteine persulfide formed from reaction 3 exhibited increased reactivity with 4,4′-dipyridyl disulfide compared to excess sodium sulfide, while Cys-S3 did not react with 4,4′-dipyridyl disulfide (Fig. 3E). Furthermore, 100 μM Cys-SS− showed increased initial rates of 4,4′-dipyridyl disulfide reduction compared to 500 μM Na2S (Fig. 3F). Similarly, glutathione
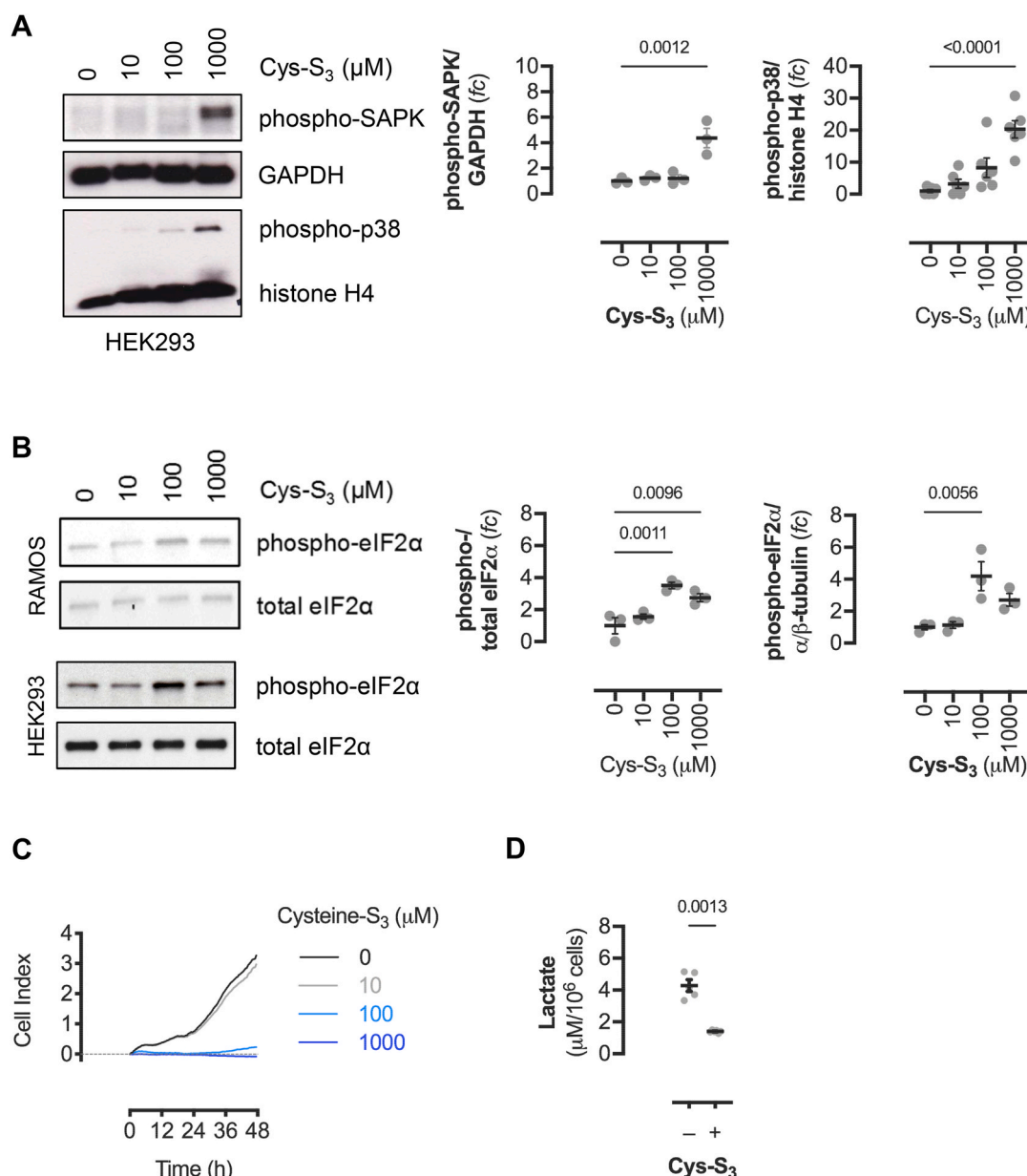
Fig. 2. Cysteine trisulfide induces cellular- and ER-stress, decreased metabolism and proliferation. Immunoblots of (A) phospho-SAPK and phospho-p38 or (B) phospho- and total eIF2α from Cys-S$_3$ treated cells for 30 min. Graphs show mean fold-change from control (±sem; n = 3–6). Significance was calculated by one-way ANOVA with Dunnett's post-hoc test. (C) Cellular proliferation measured by electrical impedance (cell index) of HEK293 cells cultured with vehicle or Cys-S$_3$. Representative data shown. (D) HEK293 lactate production after 96 h incubation with vehicle or 100 μM Cys-S$_3$ measured by ^{1}H NMR. Data shown are mean (±sem; n = 6) and significance determined by unpaired t-test with Welch's correction.

persulfide (GSS$^-$) formed from GSSG and sulfide (reaction 1) had increased nucleophilic reactivity with 4,4′-dipyridyl disulfide compared to sulfide alone (Supplemental Fig. 12).

3.4. Cysteine persulfide does not induce ER-stress and protects against electrophilic stress

Reacting Cys-S$_3$ with excess sulfide is predicted to limit the electrophilic effects of Cys-S$_3$ on cells. Cys–SS$^-$ (formed from reaction 3) or NaSH alone did not result in PKG or PTEN oxidation and cellular glutathione levels did not significantly change compared to control, whereas Cys-S$_3$ oxidized PKG and PTEN and significantly lowered reduced glutathione levels (Supplemental Fig. 13). To examine if Cys-SS$^-$ exerts ER-stress on human cells, Cys-SS$^-$ was diluted into media and cells were incubated for 30 min. Compared to Cys-S$_3$, Cys-SS$^-$ did not

induce ER-stress as measured by eIF2α phosphorylation in either RAMOS or HEK293 cells (Fig. 4A). The addition of sulfide and Cys-S$_3$ directly to the cell culture media, instead of pre-forming the equilibrium described above, did not limit eIF2α phosphorylation, indicating that the equilibrium of Reaction 3 under these conditions is shifted to the left (Supplemental Fig. 14). Consistent with the lack of protein oxidation and ER-stress, the inhibition of cellular proliferation (Fig. 4B), reduced lactate production (Fig. 4C) and altered morphology (Supplemental Fig. 15) induced by Cys-S$_3$ were not observed with Cys-SS$^-$ treatment. Interestingly, Cys–SS$^-$ did reduce cellular proliferation after 12 h compared to control and showed a modest but not statistically significant reduction in GSH levels after 1 h, suggests that persulfide donation may result in decreased cellular viability, perhaps by its electrophilic nature [35]. The ability of cysteine persulfide to limit electrophilic stress was examined using thapsigargin, a potent electrophile and inducer of
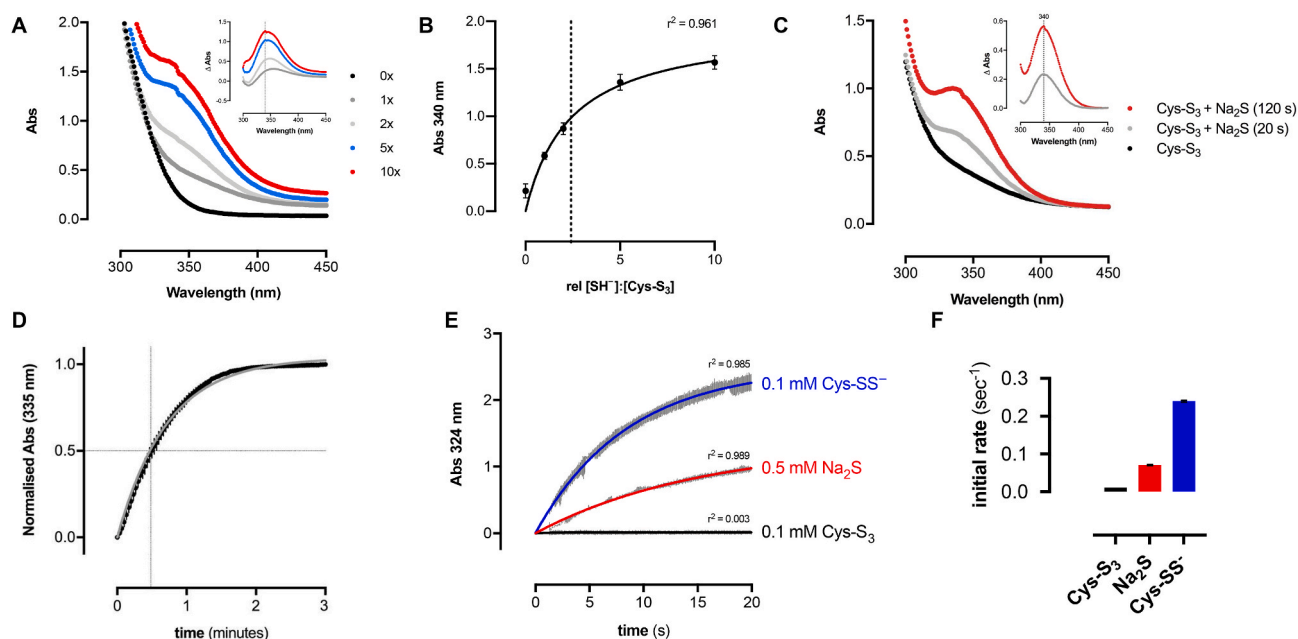
Fig. 3. Cysteine persulfide formation from the reaction of cysteine trisulfide and sodium sulfide. (A) Absorption spectra of Cys-S$_3$ (5 mM) alone or with Na$_2$S (5–50 mM). Spectra were recorded 5 min after the addition of Na$_2$S. (*inset:* the absorbance spectrum of Cys-S$_3$ subtracted from Na$_2$S + Cys-S$_3$ spectra revealing an absorption maximum at 340 nm). (B) Mean 340 nm absorbance (±sd; n = 3) of Cys-S$_3$ (5 mM) reacted with Na$_2$S (5–50 mM). Black line represents pseudo-first order regression analysis (r2 = 0.961) and KD calculated to be 2.4-fold Na$_2$S:Cys-S$_3$. (C) Absorption spectra of Cys-S$_3$ (5 mM) alone or 20 or 120 s after the addition of Na$_2$S (50 mM). (*inset:* the absorbance spectrum of Cys-S$_3$ subtracted from Na$_2$S + Cys-S$_3$ spectra). (D) Mean absorbance values (±sem; n = 6) (black) and pseudo-first order regression analysis (grey) of Cys-S$_3$ (5 mM) reacted with Na$_2$S (50 mM). (E) Kinetic analysis of 4,4′-dipyridyl disulfide reduction by Cys-S$_3$ (black), Na$_2$S (red) and Cys–SS$^-$. Data shown are mean absorbance (±sd (grey bars); n = 3). Curves represents pseudo-first order regression analyses with corresponding goodness of fit. (F) Initial rates calculated from the linear regression analysis of (E, Supplemental Fig. 6). Data shown are mean rates (−/+ sem; n = 6). (For interpretation of the references to colour in this figure legend, the reader is referred to the Web version of this article.)

ER-stress. Cells were treated with either thapsigargin alone or with Cys-SS$^-$ and ER-stress was measured by phospho-eIF2a expression. Cys-SS$^-$ effectively limited thapsigargin-induced ER-stress in both cell lines (Fig. 4D), indicating that Cys-SS$^-$ can be further utilized as a cellular protectant. Therefore, we conclude that Cys-SS$^-$ formation form Cys-S$_3$ and Na$_2$S is a method to deliver persulfides to cells without inducing widespread protein oxidation, ER stress and growth inhibition.

4. Discussion

The cellular biology of persulfides is of particular interest due to their involvement in H$_2$S signaling [4,5,20,21,35]. Persulfides are more nucleophilic and reducing, and therefore more potent anti-oxidants, than corresponding thiols [1,12]. This chemical feature of persulfides has lead to considerable interest in the formation and cellular effects of persulfides, including protein persulfide post-translational modifications and glutathione persulfide (GSS$^-$) [11,17]. Due to their reactive nature, persulfides engage in multiple equilibiria with other sulfur-species, such as H$_2$S, disulfides and polysulfides [21]. To more directly investigate persulfide biology, Cys-S$_3$ has been used as an *in situ* persulfide donor [13,24]. While Cys-S$_3$ reacts with cellular thiols to produce persulfide, the electrophilc nature of Cys-S$_3$ appears to dominate the cellular response. Our results indicate that Cys-S$_3$ paradoxically results in the generation of a strong reductant and protein oxidation. Protein thiols react with Cys-S$_3$ to form a mixed protein disulfide and cysteine persulfide (Fig. 5). As strong nucleophiles, persulfide can further react with disulfides to form a protein trisulfide and cysteine. Alternatively, Cys-S$_3$ can directly react with protein thiols to form mixed protein trisulfides, although this is likely to be a relatively very slow process [13]. The end product of either pathway is an oxidized protein thiol (*i.e.*, protein/cysteine mixed di- and trisulfides). These oxidized proteins species can further react with other reduced protein thiols to form protein aggregates linked by either intermolecular di- or trisulfide bonds. Therefore, Cys-S$_3$ results in protein oxidation, even in the presence of the strong reductant, persulfide.

The cellular response to protein oxidation and electrophilic stress is conserved throughout evolution and results in decreased proliferation and/or cytotoxicity due to necrosis or apoptosis [36–39]. Our study shows that cysteine trisulfide induced electrophilic stress and inhibited proliferation in human cell lines, similar to diallyl trisulfide and dibenzyl trisulfide [40–44]. Consistent with other reports, we show that Cys-S$_3$ can react with cellular thiols to form cysteine persulfide, a potent nucleophile and anti-oxidant [11,20]. However, we show here that Cys-S$_3$ also initiates cellular pathways that respond to electrophiles, namely p38, SAPK and eIF2α, which result in the inhibition of cellular metabolism and proliferation. We predict that many other cell signaling pathways may be altered due to trisulfide or persulfide donation. Therefore, we conclude that Cys-S$_3$ administration to cells can deliver cysteine persulfide *in situ*, however this is concomitant with protein oxidation and cytotoxicity, consistent with other dialkyl and diaryl trisulfide compounds [43–45]. Our findings are counter to recent reports on the cellular protective effects of Cys-S$_3$ at similar concentrations in *E. coli* and human cells [13,24], however differing experimental design and conditions may account for some of this discrepancy.

While we observed significant thiol oxidation by Cys-S$_3$, trisulfides can have different modes of reactivity. For example, trisulfides can react with electrophiles via a hydrolysis-assisted mechanism [46]. Furthermore, Cys-S$_3$ could inhibit the mitochondrial electron transport chain, which may contribute to the cytotoxic nature of Cys-S$_3$ similar to sodium tetrasulfide [47]. These alternate routes of reactivity further confound the use of Cys-S$_3$ as an *in vivo* or *in vitro* persulfide donor.

Interestingly, cystine (cysteine disulfide; Cys-S-S-Cys) is essential for *in vitro* cellular growth and is present in many common cell culture media at 200 μM. Cys-S$_3$ is structurally similar, yet is toxic to cells at 100
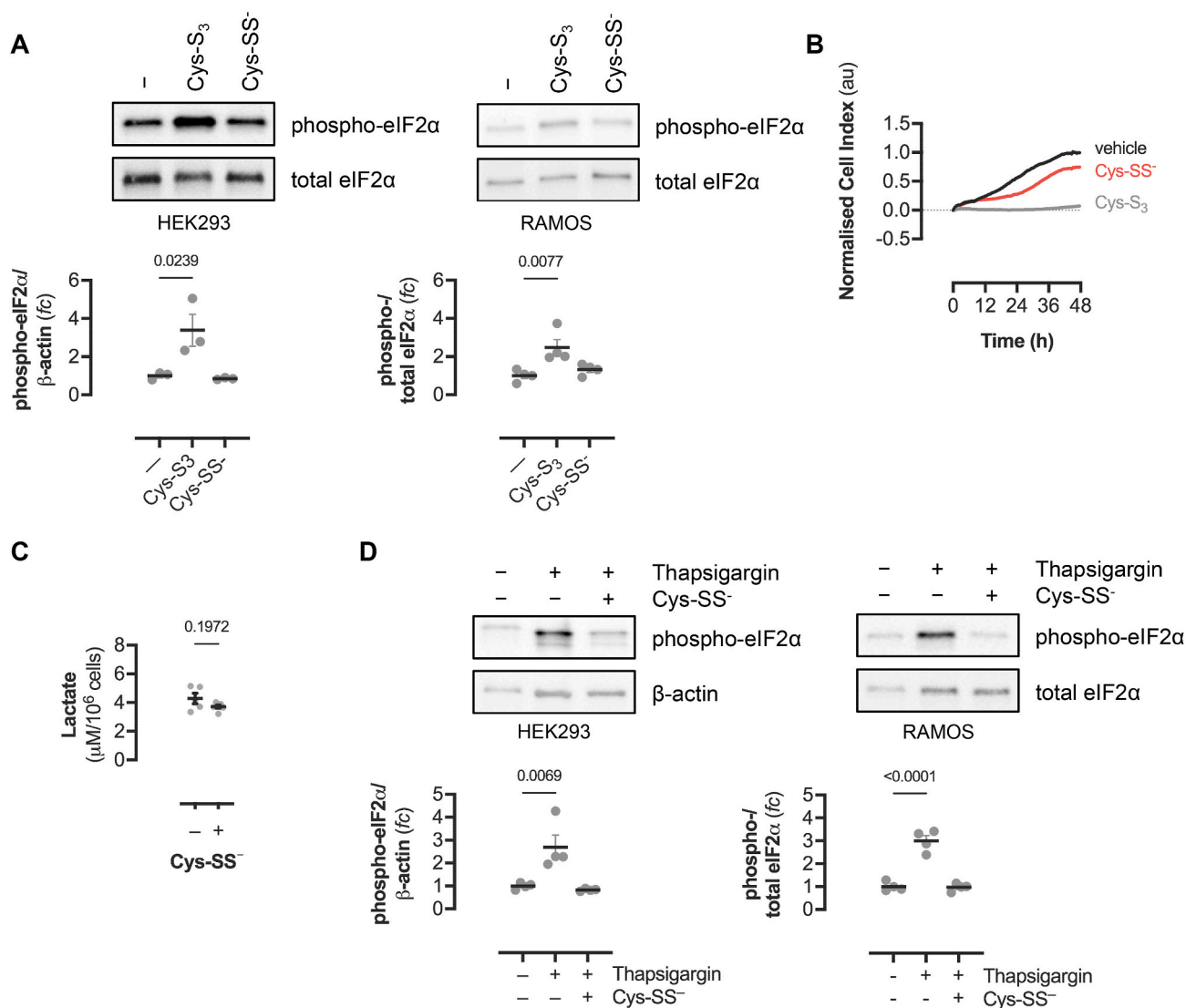
Fig. 4. Cysteine persulfide protects cells from electrophilc stress. (A) Immunoblot of phospho- and total eIF2a from cells treated with either Cys-S$_3$ or Cys–SS$^-$ for 30 min. Graphs show mean normalized fold-change from controls (±sem; n = 3–4). Significance was calculated by one-way ANOVA with Dunnett's post-hoc test. (B) Cellular proliferation measured by electrical impedance (cell index) of HEK293 cells cultured with vehicle (black), Cys–SS$^-$ (red) or Cys-S$_3$ (grey). (C) HEK293 lactate production after 96 h incubation with vehicle or Cys–SS$^-$ measured by ^{1}H NMR. Data shown are mean (±sem; n = 6) and significance determined by unpaired *t*-test with Welch's correction. (D) Immunoblot of phospho- and total eIF2α from cells treated with thapsigargin (1 μM) alone or with Cys–SS$^-$ (100 μM). Graphs show mean normalized fold-change from controls (±sem; n = 4). Significance was calculated by one-way ANOVA with Dunnett's post-hoc test. (For interpretation of the references to colour in this figure legend, the reader is referred to the Web version of this article.)
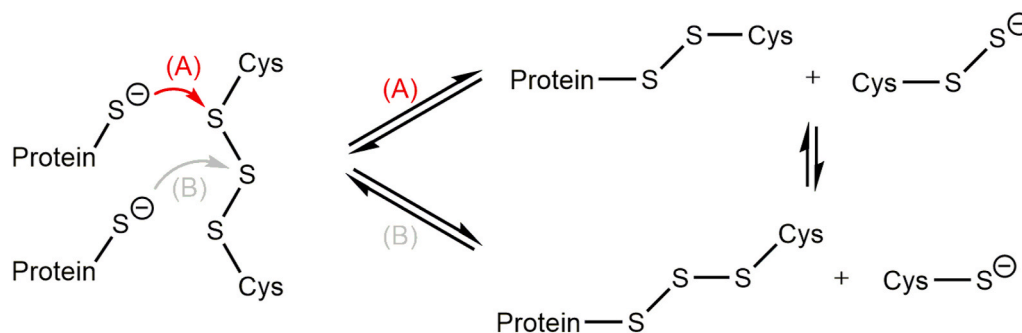

Fig. 5. Cysteine trisulfide results in protein thiol oxidation. Protein thiols react with cysteine trisulfide to form cysteine persulfde and a mixed protein-cysteine disulfide (A). Persulfide can then react with the disulfide to form cysteine and protein-cysteine trisulfide. Alternatively, protein thiols can react to directly form cysteine and protein-cysteine trisulfide (B), although this is predicted to be slow compared to (A).

μM. It is surprising that the addition of one S atom to cystine induces protein oxidation and cell stress and strongly indicates that trisulfides or persulfide formation has additional biological effects compared to disulfides. Persulfide/polysulfide generating enzymes, such as cysteinyl-tRNA synthetases, control mitochondrial energy production [8]; however additional intracellular signaling from these enzymes is expected and the electrophilic sensing pathways described here among others may be downstream effectors of these enzymes. The inhibition of cell growth observed here suggests that Cys-S_3 could have potential as an anti-cancer therapy. A similar trisulfide derived from garlic, diallyl trisulfide, inhibits cell cycle progression and induces apoptosis in cancer cells [44,45,48]. Additionally, dibenzyl trisulfide limits neuroblastoma cell growth [43]. Here we show that cysteine trisulfide inhibits cell proliferation similar to other trisulfides, suggesting that cysteine trisulfide may have comparable anti-cancer effects.

While ER-stress is often associated with increased reducing capacity, it is clear that electrophiles also induce ER stress [34], as prototypical ER-stress inducers such as thapsigargin and tunicamycin are classic Michael acceptors. An alternative mechanism for the promotion of ER-stress by Cys-S_3 is the persulfidation of PTP1B, which would results in increased eIF2a phosphorylation and decreased protein synthesis [18], however we did not examine this possibility. In an attempt to eliminate the electrophilic stress induced by Cys-S_3 while retaining persulfide donation, sodium sulfide was used to generate persulfide at high pH. Given that the reverse of Reaction 3 would be dependent on proton concentration, the reaction was done at high pH to favor the formation of persulfide anion and to limit the back reaction. While the combination of Cys-S_3 and sulfide protected against thapsigargin-induced ER-stress, the exact species responsible for this is not clear due to the complex equilibria present [7,16,21].

A major limitation of our study is the presence of excess sulfide in the preparation of Cys-SS$^−$. H_2S can alter the complex equilibria of thiol/sulfide-related species and the results of this mixture can be difficult to interpret and therefore we do not recommend this method for the *in situ* generation of persulfides. Reacting Cys-S_3 with other thiols such as glutathione would avoid the presence of excess sulfide, however this method would generate equimolar persulfide and disulfide. Therefore, it appears that persulfide formation from Cys-S_3 has limitations from either protein oxidation and cellular stress or the presence of confounding thiol species. Despite the limitations of Cys-S_3 described here, persulfides are still an interesting aspect of sulfur biochemistry to elucidate and the utility of other persulifde donors, such as alkylsulfenyl thiocarbonates [49], should be thoroughly investigated. In conclusion, cysteine trisulfide rapidly reacts with thiols to form cysteine persulfide, however in a cellular context, trisulfide-mediated thiol oxidation initiates signaling pathways that dominate the observed cellular effect, despite the formation cysteine persulfide.

Declaration of competing interest

The authors have no competing interests to declare.

Acknowledgements

Appendix A. Supplementary data

Supplementary data to this article can be found online at https://doi.org/10.1016/j.redox.2021.102155.

Funding

References

[1] N.E. Francoleon, S.J. Carrington, J.M. Fukuto, The reaction of H2S with oxidized thiols: generation of persulfides and implications to H2S biology, Arch. Biochem. Biophys. 516 (2) (2011) 146–153.

[2] C. Hine, et al., Endogenous hydrogen sulfide production is essential for dietary restriction benefits, Cell 160 (1–2) (2015) 132–144.

[3] Y. Zhang, et al., Hydrogen sulfide, the next potent preventive and therapeutic agent in aging and age-associated diseases, Mol. Cell Biol. 33 (6) (2013) 1104–1113.

[4] B.D. Paul, S.H. Snyder, H(2)S signalling through protein sulfhydration and beyond, Nat. Rev. Mol. Cell Biol. 13 (8) (2012) 499–507.

[5] M.R. Filipovic, et al., Chemical biology of H2S signaling through persulfidation, Chem. Rev. 118 (3) (2018) 1253–1337.

[6] G.S. Rao, G. Gorin, Reaction of cystine with sodium sulfide in sodium hydroxide solution, J. Org. Chem. 24 (6) (1959) 749–753.

[7] P.K. Yadav, et al., Biosynthesis and reactivity of cysteine persulfides in signaling, J. Am. Chem. Soc. 138 (1) (2016) 289–299.

[8] T. Akaike, et al., Cysteinyl-tRNA synthetase governs cysteine polysulfidation and mitochondrial bioenergetics, Nat. Commun. 8 (1) (2017) 1177.

[9] T. Ida, et al., Reactive cysteine persulfides and S-polythiolation regulate oxidative stress and redox signaling, Proc. Natl. Acad. Sci. Unit. States Am. 111 (21) (2014) 7606.

[10] J.O. Edwards, R.G. Pearson, The factors determining nucleophilic reactivities, J. Am. Chem. Soc. 84 (1) (1962) 16–24.

[11] D. Benchoam, et al., Acidity and nucleophilic reactivity of glutathione persulfide, J. Biol. Chem. 295 (46) (2020) 15466–15481.

[12] R. Millikin, et al., The chemical biology of protein hydropersulfides: studies of a possible protective function of biological hydropersulfide generation, Free Radic. Biol. Med. 97 (2016) 136–147.

[13] C.L. Bianco, et al., The reaction of hydrogen sulfide with disulfides: formation of a stable trisulfide and implications for biological systems, Br. J. Pharmacol. 176 (4) (2019) 671–683.

[14] C.L. Bianco, et al., The chemical biology of the persulfide (RSSH)/perthiyl (RSS.) redox couple and possible role in biological redox signaling, Free Radic. Biol. Med. 101 (2016) 20–31.

[15] S. Kasamatsu, et al., Redox signaling regulated by cysteine persulfide and protein polysulfidation, Molecules 21 (12) (2016) 1721.

[16] K. Ono, et al., Redox chemistry and chemical biology of H2S, hydropersulfides, and derived species: implications of their possible biological activity and utility, Free Radic. Biol. Med. 77 (2014) 82–94.

[17] E. Doka, et al., Control of protein function through oxidation and reduction of persulfidated states, Sci. Adv. 6 (1) (2020), eaax8358.

[18] N. Krishnan, et al., H2S-Induced sulfhydration of the phosphatase PTP1B and its role in the endoplasmic reticulum stress response, Sci. Signal. 4 (203) (2011) ra86-ra86.

[19] J. Westley, et al., The sulfurtransferases, Fund. Appl. Toxicol. 3 (5) (1983) 377–382.

[20] L. Alvarez, et al., Chemical biology of hydropersulfides and related species: possible roles in cellular protection and redox signaling, Antioxidants Redox Signal. 27 (10) (2017) 622–633.

[21] J.M. Fukuto, et al., Biological hydropersulfides and related polysulfides - a new concept and perspective in redox biology, FEBS Lett. 592 (12) (2018) 2140–2152.

[22] D.M. Miller-Martini, S. Hua, P.M. Horowitz, Cysteine 254 can cooperate with active site cysteine 247 in reactivation of 5,5'-dithiobis(2-nitrobenzoic acid)-inactivated rhodanese as determined by site-directed mutagenesis, J. Biol. Chem. 269 (17) (1994) 12414–12418.

[23] J. Lin, et al., The uptake and release of polysulfur cysteine species by cells: physiological and toxicological implications, Chem. Res. Toxicol. 32 (3) (2019) 447–455.

[24] C.F. Henderson, et al., Cysteine trisulfide protects E. coli from electrophile-induced death through the generation of cysteine hydropersulfide, Chem. Res. Toxicol. 33 (2) (2020) 678–686.

[25] S. Kim, et al., Keap1 cysteine 288 as a potential target for diallyl trisulfide-induced Nrf2 activation, PloS One 9 (1) (2014), e85984.

[26] E.A. Veal, et al., A 2-Cys peroxiredoxin regulates peroxide-induced oxidation and activation of a stress-activated MAP kinase, Mol. Cell. 15 (1) (2004) 129–139.

[27] R. Bassi, et al., Redox-dependent dimerization of p38alpha mitogen-activated protein kinase with mitogen-activated protein kinase kinase 3, J. Biol. Chem. 292 (39) (2017) 16161–16173.

[28] D.K. Hill, et al., 1H NMR and hyperpolarized 13C NMR assays of pyruvate–lactate: a comparative study, NMR Biomed. 26 (10) (2013) 1321–1325.

[29] E. Cuevasanta, et al., Reaction of hydrogen sulfide with disulfide and sulfenic acid to form the strongly nucleophilic persulfide, J. Biol. Chem. 290 (45) (2015) 26866–26880.

[30] J.R. Burgoyne, et al., Cysteine redox sensor in PKGIa enables oxidant-induced activation, Science 317 (5843) (2007) 1393–1397.

[31] S.-R. Lee, et al., Reversible inactivation of the tumor suppressor PTEN by H2O2*, J. Biol. Chem. 277 (23) (2002) 20336–20342.

[32] D. Giustarini, et al., S-glutathionylation: From redox regulation of protein functions to human diseases, J. Cell Mol. Med. 8 (2) (2004) 201–212.

[33] J.V. Cross, D.J. Templeton, Regulation of signal transduction through protein cysteine oxidation, Antioxidants Redox Signal. 8 (9–10) (2006) 1819–1827.

[34] N. Takasugi, et al., The emerging role of electrophiles as a key regulator for endoplasmic reticulum (ER) stress, Int. J. Mol. Sci. 20 (7) (2019) 1783.

[35] D. Benchoam, et al., Persulfides, at the crossroads between hydrogen sulfide and thiols, Essays Biochem. 64 (1) (2020) 155–168.

[36] Y. Kumagai, Y. Abiko, Environmental electrophiles: protein adducts, modulation of redox signaling, and interaction with persulfides/polysulfides, Chem. Res. Toxicol. 30 (1) (2017) 203–219.

[37] A. van der Vliet, et al., Cellular and environmental electrophiles: balancing redox signaling, inflammation, and cell death pathways, in: G. Valacchi, P.A. Davis (Eds.), Oxidants in Biology: A Question of Balance, Springer Netherlands, Dordrecht, 2008, pp. 37–66.

[38] J. Han, et al., ER-stress-induced transcriptional regulation increases protein synthesis leading to cell death, Nat. Cell Biol. 15 (5) (2013) 481–490.

[39] S. Orrenius, V. Gogvadze, B. Zhivotovsky, Mitochondrial oxidative stress: implications for cell death, Annu. Rev. Pharmacol. Toxicol. 47 (1) (2007) 143–183.

[40] M. Murai, et al., Diallyl trisulfide sensitizes human melanoma cells to TRAIL-induced cell death by promoting endoplasmic reticulum-mediated apoptosis, Int. J. Oncol. 41 (6) (2012) 2029–2037.

[41] H.C. Wang, et al., Diallyl trisulfide induces apoptosis of human basal cell carcinoma cells via endoplasmic reticulum stress and the mitochondrial pathway, Nutr. Canc. 64 (5) (2012) 770–780.

[42] J. Zheng, et al., Diallyl trisulfide induces G2/M cell-cycle arrest and apoptosis in anaplastic thyroid carcinoma 8505C cells, Food Funct 10 (11) (2019) 7253–7261.

[43] H. Rosner, et al., Disassembly of microtubules and inhibition of neurite outgrowth, neuroblastoma cell proliferation, and MAP kinase tyrosine dephosphorylation by dibenzyl trisulphide, Biochim. Biophys. Acta 1540 (2) (2001) 166–177.

[44] X.Y. Jiang, et al., Diallyl trisulfide suppresses tumor growth through the attenuation of Nrf2/Akt and activation of p38/JNK and potentiates cisplatin efficacy in gastric cancer treatment, Acta Pharmacol. Sin. 38 (7) (2017) 1048–1058.

[45] A.A. Powolny, S.V. Singh, Multitargeted prevention and therapy of cancer by diallyl trisulfide and related Allium vegetable-derived organosulfur compounds, Canc. Lett. 269 (2) (2008) 305–314.

[46] T. Sawa, et al., Chemical Biology of Reactive Sulfur Species: Hydrolysis-Driven Equilibrium of Polysulfides as a Determinant of Physiological Functions, Antioxidants Redox Signal. (2021).

[47] T. Uba, et al., Polysulfide inhibits hypoxia-elicited hypoxia-inducible factor activation in a mitochondria-dependent manner, Mitochondrion 59 (2021) 255–266.

[48] M.T. Puccinelli, S.D. Stan, Dietary bioactive diallyl trisulfide in cancer prevention and treatment, Int. J. Mol. Sci. 18 (8) (2017).

[49] V.S. Khodade, et al., Alkylsulfenyl thiocarbonates: precursors to hydropersulfides potently attenuate oxidative stress, Chem. Sci. 12 (23) (2021) 8252–8259.